Integrated risk assessment due to slope instabilities at the roadway network of Gipuzkoa, Basque Country

Olga Mavrouli [1], Jordi Corominas [2], Iñaki Ibarbia[3], Nahikari Alonso[4], Ioseba Jugo[3], Jon Ruiz[4], Susana Luzuriaga[5] and José Antonio Navarro[5]

[1] Faculty of Geo-Information Science and Earth Observation (ITC), University of Twente, Enschede, Netherlands; previously at Department of Civil and Environmental Engineering, Technical University of Catalonia, BarcelonaTech (UPC)

[2] Department of Civil and Environmental Engineering, Technical University of Catalonia, BarcelonaTech (UPC)
[3] Ikerlur, S.L., Donostia
[4] LKS Ingeniería, S. Coop., Arrasate/Mondragon
[5] Diputación Foral de Gipuzkoa-Gipuzkoako Foru Aldundia, Donostia/San Sebastián
Correspondence to: o.c.mavrouli@utwente.nl & jordi.corominas@upc.edu

Abstract. Transportation corridors such as roadways are often subjected to both natural instability and cut slope failures, with substantial physical damage for the road infrastructure and threat to the circulating vehicles and passengers. In the early 2000s, the Gipuzkoa Regional Council of the Basque country in Spain, marked the need for assessing the risk related to the geotechnical hazards at its road network, in order to assess and monitor their safety for the road users. The Quantitative Risk Assessment (QRA) was selected as a tool for comparing the risk for different hazards on an objective basis. Few examples of multi-hazard risk assessment along transportation corridors exist. The methodology presented here consists in the calculation of risk in terms of probability of failure and its respective consequences, and it was applied to 84 selected points of risk (PoR) of the entire road network managed by the Gipuzkoa Regional Council. The types of encountered slope instabilities which are treated are rockfalls, retaining wall failures, and slow moving landslides. The proposed methodology includes the calculation of the probability of failure for each hazard based on an extensive collection of field data, and its association with the expected consequences. Instrumentation data from load cells for the anchored walls and inclinometers for the slow moving landslides was used. The expected road damage was assessed for each hazard level in terms of a fixed Unit Cost, UC. The results indicate that the risk can be comparable for the different hazards. 21% of the PoR in the study area were found to be of very high risk.

1. Introduction

Transportation corridors such as roadways are often subjected to both natural instability and cut slope failures, with substantial physical damage for the road infrastructure and threat to the circulating vehicles and passengers.

The growing societal demand for road safety requires managing this risk, and places a high priority on the identification of problematic areas, to effectively manage the mitigation works.

Risk is most commonly conceptualized as the product of hazard, exposure, and vulnerability. Qualitative risk analysis for transportation corridors traditionally combines different levels of hazard and vulnerability to provide the risk across a network (e.g. Pellicani et al. 2017). Nevertheless, the interpretation of risk levels which are obtained qualitatively may vary for the different hazards (Eidsvig et al. 2017). The homogenization of the risk for multi-hazards remains a challenge because of the variability in the nature of soil or rock mass movement phenomena and the difference in the type and extent of the consequences. The comparison of different types of geotechnical risks in roadways, such as slope movements and retaining structures failure, requires bringing these phenomena under a common denominator. Quantitative risk descriptors, as being objective expressions of the expected risk extent, may well serve for the homogenization of the risk levels for different hazards and types of exposed elements (persons, vehicles, infrastructure, and indirect economical loss). Common quantitative risk descriptors are the expected annual monetary loss, the probability of a given loss scenario, the probability of one or more fatalities, and others mentioned at Corominas et al. (2014).

One of the major limitations for the quantitative risk assessment in roadways is the great data demand that it implies. The hazard in terms of probability of an event of a given magnitude requires extensive data on the frequency and also magnitude (volume) of the events (Fell et al., 2008; Jaiswal et al. 2010). Most commonly, landslide inventories are required (Dai et al., 2002; Ferlisi et al. 2012), although in most cases they are scarce. Highway and traffic administration authorities are potential data providers (Hungr et al., 1999), however complete and reliable maintenance records are rarely kept and made available. Alternative methods to overcome the scarcity of empirical data are provided at Corominas et al. (2014), and they are based on geomechanical or indirect approaches. They associate the occurrence of events with the temporal occurrence of their triggering factors, such as the return period of a rainfall of a given intensity. On the other hand, for a purely quantitative risk assessment, the calculation of the consequences in terms of realistic expected costs is a challenge, as the amount of repair or insurance expenses fluctuates greatly depending on the type and extent of the damage, on top of the indirect costs related to traffic interruptions, detours and further loss related to traffic accidents. Due to these limitations, few purely quantitative multi-hazard risk assessments for roadways exist in the literature.

An extensive review of highway slope instability risk assessment systems is provided by Pantelidis (2011), including several qualitative and semi-quantitative methods (here by semi-quantitative we refer to the methodologies that assess the hazard in terms of numerical scores). A well-known example of semi-quantitative methods is the Rockfall Hazard Rating System (Pierson and Van Vickle, 1993) recommended by the FHWA (Federal Highway Administration of the United States), which was later adapted by Budetta (2004), specifically for rockfall risk along roads. The pure quantitative risk assessment (QRA) however consists in the hazard assessment in terms of probability of failure/occurrence of an event of a given magnitude multiplied with its respective consequences (Fell et al. 2008), which is not treated by semi-quantitative methods.

Hungr et al. (1999) quantified the rockfall risk along roadways at the British Columbia, after deriving magnitude-cumulative frequency curves. Bunce et al. (1997) were amongst the first to use the roadway damage in order to assess the rock fall frequency. Remondo et al. (2008) proposed a method for the quantification of the damage at the Gipuzkoa road network where losses were calculated on the basis of past damage records and taking into account budgets for road and railway track repairs. Similarly, Zêzere et al. (2008) assessed the direct risk from translational, rotational and shallow landslides in the north of Lisbon, Portugal, employing road reconstruction costs within a Geographical Information System. Ferlisi et al. (2012) using the fundamental risk equation provided by Fell et al. (2008) calculated the annual probability of one or more fatalities by rockfalls in the Amalfi coastal road, Southern Italy, and Michoud et al. (2012) presented an example from the Swiss Alps. Jaiswal et al. (2010) applied a risk model for debris slides, where the temporal probability was indirectly obtained by the return period of the triggering rainfalls and the road vulnerability was assessed in function of the road location and expected debris magnitude. Ferrero and Migliazza (2013) made a first attempt to incorporate the efficiency of protection measures into the risk assessment (Nicolet et al. 2016). Still, when it comes to the practical application of quantitative risk analysis to linear infrastructures, several challenges exist.

One of the most important is the assessment of the expected magnitude-frequency relations and of the annual probability of occurrence for a hazard of a certain magnitude/intensity, in particular where past event inventories are incomplete or missing. As afore-mentioned, alternative methods have been suggested to this end, however in most cases their application is limited to site specific. There is a scarcity of cost-efficient, quick, simple and easy enough methodologies, to be applied to extensive road networks, using as input the evidences that can be found in the vicinity of the transportation corridors, field inspections or instrumentation. Given those limitations, the determination of landslide magnitude-frequency data requirements and its specifications, within a suitable and feasible framework for transportation corridors, remains an issue.

Assessing the condition of assets such as road pavements and protection infrastructure (in this case retaining walls) allows for monitoring operational efficiency, planning future maintenance and rehabilitation activities and controlling costs, through condition forecasting models (Gharaibeh and Lindholm, 2014). Although models for predicting pavement deterioration under usual stress conditions have been used for more than three decades now, literature is lacking prediction models for disruptive slope instability events. Similarly, simple yet functional and (semi)quantitative-based empirical models for the condition assessment of retaining walls are scarce.

Diverse hazards types require different descriptors for predicting asset condition. In quantitative multi-hazard risk assessment, the use of all descriptors should produce comparable results at a common and meaningful (commonly financial) scale. This requires, in each case, adequate criteria and thresholds for the establishment of hazard classes, to associate with vulnerability levels and costs (Schmidt et al. 2011; Kappes et al. 2012). Very few examples of roadway vulnerability exist in the literature (e.g. Mansour et al. 2011; Eidsvig et al. 2017). Their applicability or adjustment to other case-studies is a topic for further research.

The work that is presented here aims at filling in these gaps for the development of a comprehensive procedure including suitable data collection, hazard and vulnerability assessment and their integration into risk calculations. Up to date and to the authors' knowledge there are scarce integrated approaches for multi-hazard quantitative risk analysis at transportation routes, at site-specific and local scale. The starting point was the need for a risk assessment system for a specific area, and all approaches discussed here for confronting these issues are strongly related to the local characteristics of the study-area and the available documentation and instrumentation.

In particular, in the early 2000s, the Gipuzkoa Regional Council of the Basque Country in Spain, marked the need for assessing the risk related to the geotechnical hazards at its road network, in order to assess and monitor their safety for the road users. The main objective has been the identification of the most problematic areas where mitigation measures should be prioritized. In that specific road network, a variety of geotechnical hazards coexist, which are relevant to both cut and natural slope instabilities, and including the potential failure of retaining walls. A quantitative risk analysis approach was proposed.

The methodology presented here was developed with the objective to compare the risk levels, for a variety of elements comprising roads and retaining walls, using a common unique criterion for their evaluation. It consists in the quantitative risk assessment (QRA) in terms of probability of failure and its respective consequences, at 84 selected points of risk (PoR) of the entire road network managed by the Gipuzkoa Regional Council (Fig. 1). The types of encountered slope instabilities which are treated in this manuscript are rockfalls, retaining walls, and slow moving landslides. Further geotechnical risks in the area include debris flows, instability of embankments and brittle slope failures, but their assessment is not included here.

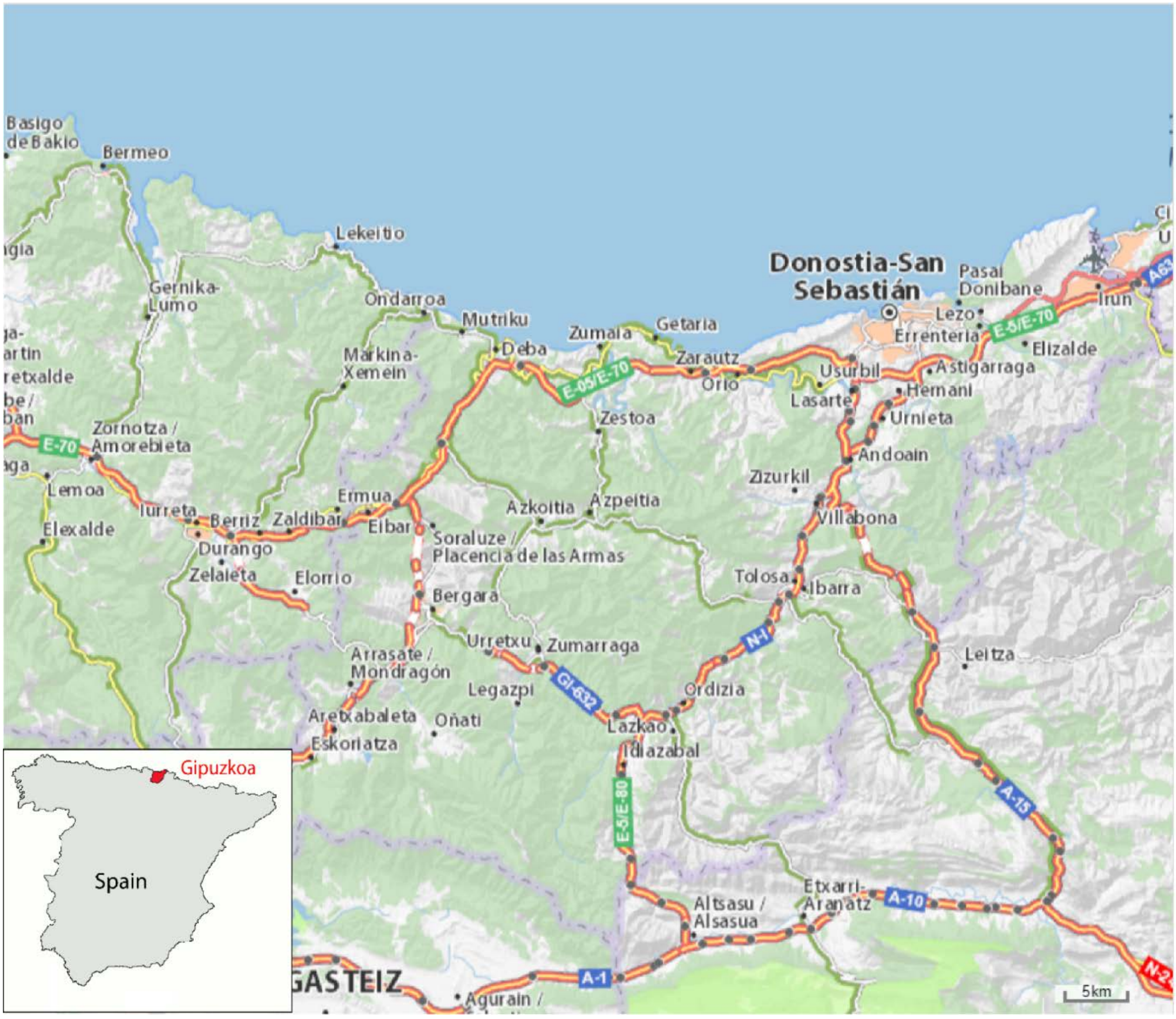

Figure 1: Road network managed by the Gipuzkoa Regional Council (map source ViaMichelin website at https://www.viamichelin.com/web/Maps, last accessed in September 2018).

2. Study area and data availability

The study area is the road network managed by the Gipuzkoa Road Authority, in the Basque Country, Spain (Fig. 1). It consists of four networks: highways, primary, county, and local roads. Their difference lies in their capacity and function as connecting corridors between major and/or minor urban/rural nuclei. In that region, the layout of the road network has been spatially constrained since its design by its characteristically intense morphological relief. Soil infills or excavations and important constructions such as retaining walls are required to protect the road users and the road infrastructure against soil/rock mass movements and instabilities. An important fraction of the retaining walls is anchored walls.

From a geological point of view, the Gipuzkoa province is part of the Basque-Cantabrian basin (Barnolas and Pujalte, 2004). More specifically, it is the segment connecting the Pyrenees and the Cantabrian mountains to the West (Tugend et al. 2014). It experienced normal faulting and high subsidence rates during the Cretaceous and was inverted during Tertiary compression related to the Alpine orogeny (Gómez et al. 2002). The outcropping rocks cover a wide temporal record, from the Upper Paleozoic to the Quaternary. However, there is no representation of the materials belonging to the period between the Lower-Middle Tertiary (Oligocene) and Early Pleistocene. The geology of the study area is well synthetized by Ábalos (2016) (Fig. 2).

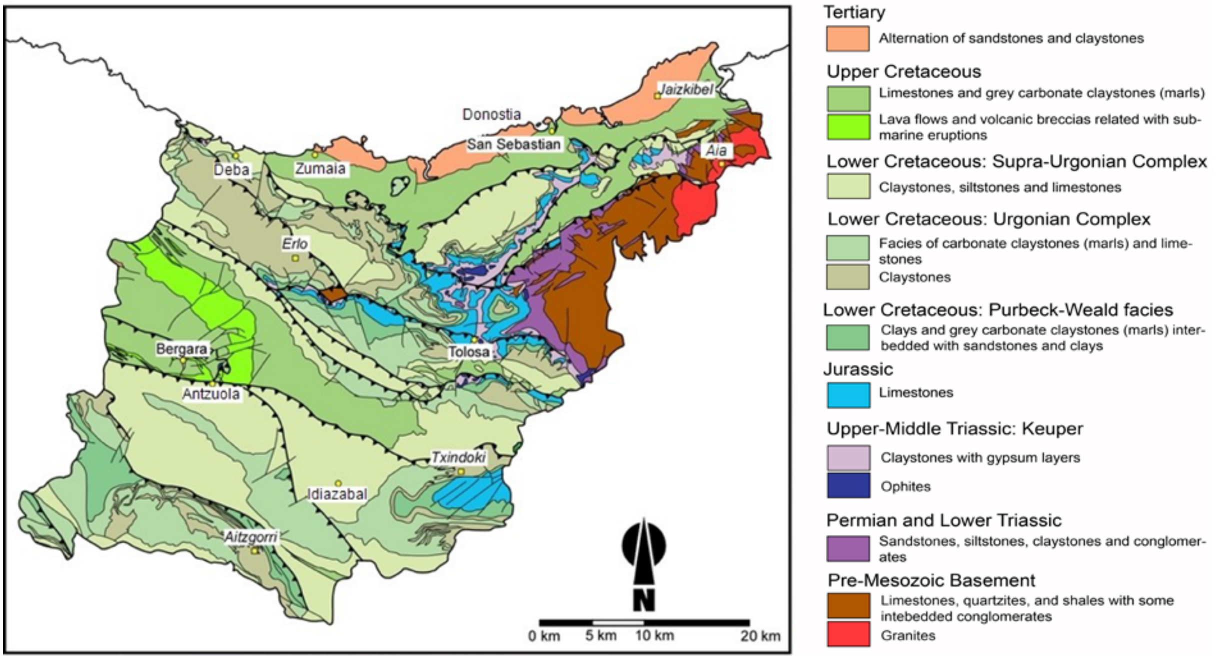

Figure 2: Geological sketch of Gipuzkoa province (modified from Ábalos, 2016).

According to it, two well differentiated geological sectors can be distinguished. The first one extends over the NE corner of Gipuzkoa, in which the Paleozoic rocks (granitoid rocks and limestone layers overlaid by quartzites and shales with some interbedded conglomerate layers) and Triassic rocks (sandtones, siltstones, claystones and conglomerates) are predominant. The rest of the Gipuzkoa province is composed of thick sedimentary assemblages, mainly Cretaceous and Tertiary (Fig. 2). The outcropping lithological units are diverse. Jurassic rocks are usually composed of carbonate rocks of marine platform facies. Several stratigraphic units are found in the Lower Cretaceous formations. The Weald complex is composed of continental and freshwater sedimentary rocks. The Urgonian complex is formed by reefal limestones; the Supra-Urgonian Complex exhibits a considerable internal complexity, mostly clayey limestones, siltstones, and argillites. The Upper Cretaceous is characterized by Flysch alternations and Tertiary flyschoid sandstones. In general, the sedimentary rocks were formed in a great diversity of depositional environments, although they mostly correspond to marine environments, with intercalations of continental or transitional facies.

Materials such as limestones, conglomerates, and sandstones stand out and form the topographic relief, as being more resistant to erosion than the clay and siltstone zones, which are also present in the area.

Concerning tectonics, all the aforementioned materials appear folded and fractured as a result of actions during the two orogenic phases. The oldest one, corresponding to the hercynian orogeny, affected the Paleozoic rocks while the more recent alpine orogeny has been the responsible for the general uplift of the Pyrenean Mountain Range. During the uplift, the Mesozoic sedimentary cover detached from the Paleozoic basement, in favour of the most deformable lithological units (e.g. Keuper), and created a complex structure of folds faults and diapirs. Both the folds and the main fractures have alignments oriented in the direction NE-SE and NW-SE, which in the eastern part of the Gipuzkoa province form an arch that bounds the Paleozoic reliefs.

The Quaternary rock deposits pertain to residual soils, originating from the disintegration, weathering or dissolution of the underlying rock mass, without having undergone transport (colluvium, scree deposits on the foot of steep slopes), and alluvial soils.

Since 2002, the Department of Mobility and Road Infrastructure of Gipuzkoa developed and installed an extensive system for the surveillance and monitoring of the anchored retaining walls with hydraulic or vibrating wire load cells, placed over the most representative and critical retaining structures and slopes. The monitoring system is completed with further instrumentation of the slopes and embankments, comprising piezometers, inclinometers measuring quarterly to semi-annual displacement, and extensometers, controlling, on a continuous basis, 100 Points of Risk (PoR). 84 points of them involve rockfalls (20 PoR), potentially unstable anchored retaining walls (37 PoR), and slow moving landslides (27 PoR). In spite of the instrumentation data available in the area, the comparison of the risk levels at the different PoR and the establishment of a methodology for the homogenous multi-hazard quantitative risk assessment have remained unresolved until the proposal of the methodology that is presented here.

Five road types based on the Average Daily Traffic (ADT) can be distinguished (Table 1), for which the geotechnical hazard situations vary. For the sake of brevity, only the three aforementioned types of instability are treated here. Typical examples of them in the study area are shown in Section 4. In particular, the different hazard situations can be summarized as follows:

- Rockfalls with or without mitigation measures (RF);
- Anchored walls partially or totally instrumented with inclinometers and/or load cells inspected on a continuous or annual basis (RS);
- Instrumented slow moving landslides with available geotechnical study (SL).

Table 1: Occurrence of geotechnical hazard types at different road types (data source: Department of Mobility and Road Infrastructure of Gipuzkoa).

Road Type	ADT	Networks	Anchored walls	Rockfalls	Slow moving landslides
1	>25,000	Highway / Primary	x		x
2	15,000-25,000	Highway / Primary	x	x	x
3	5,000-15,000	Highway/Primary / County	x	x	x
4	1,000-5,000	Primary / County / Local	x	x	x
5	<1,000	County / Local		x	x

ADT: Average Daily Traffic

Rainfall data has been available for the study site by the Meteorological Agency of the Basque country. Further data has been collected after periodical field inspections and from the monitoring network, the type of which differs according to the hazard. This is detailed in the following section. Periodic inspections have been on-going, up to date.

3. General Methodology for the Risk Assessment

The objective of the general methodology that is presented here is to compare, on a common basis, the risk at the different PoR. The risk components that are used are the hazard and the consequences. For the calculation of the risk, the methodology takes into account the repair of damage in order to restore normal traffic. This expresses the direct risk for the road. The risk quantification in terms of monetary loss requires calculating repair costs for different damages for each hazard, as described in Table 13 (Appendix). Indirect loss such as the economic impact of the road blockage and detours, although it might be substantial, is not described here.

The hazard is expressed in terms of annual probability of failure of a natural/cut slope or retaining wall, of a given magnitude j. Magnitude (volume) or intensity (velocity) descriptors were defined for each hazard. Different procedures were used to assess the annual probability of an event of a given magnitude or intensity for the processes that are presented in the next sections. For dormant landslides, the probability of a sudden reactivation was assessed. The consequences include costs related to removal of rubble, repair/replacement of the pavement, scaling of the slopes (the removal of loose non detached rock or debris), and slope stabilization. The cost is evaluated in multiples of a Unit Cost, UC, set at 1,000 €.

If more than one types of hazards are present on a given PoR, the total risk is the sum of risks.

The overall methodology for the quantification of the risk consists in the general application of Eq. (1).

$$\mathrm{R_T} = \sum_{\mathrm{j}}^{\mathrm{k}} \mathrm{P_{rk}} * C_k \, , \tag{1}$$

Where:

R_T: Average annual risk in terms of UC per year

j: Magnitude (volume) or intensity (velocity) class

k: Hazardous event type (rockfall; failure of an anchored retaining wall; slow moving landslide)

P_r: Annual probability/frequency of occurrence of a failure/rupture of magnitude j. For slow moving landslides, it refers to the probability of acceleration of a landslide with a given level of intensity (velocity).

C_k: Consequences of the failure/rupture caused by a hazardous k-type event of magnitude j, in terms of multiples of the UC (set at 1,000 €).

The magnitude classes of the adverse events are established empirically based on the observed consequences (road damage) and the average cost of the remedial measures typically undertaken (see Appendix).

For each hazard, further assumptions are made and steps are followed for the evaluation of the components of Eq. (1), which are described in the following sections.

3.1 Rockfalls (RF)

Rockfalls are a major threat at the roads of Gipuzkoa. The rockfall hazard magnitude is classified according to the volume of the detached mass. Figure 3 shows representative examples of different rockfall magnitudes. A frequency or probability of occurrence is attributed to each volume class and the extent of disruption of the transportation corridor is determined.

For the frequency-magnitude relation, a catalogue of events is available only for limited sections of the road network. An inventory of rockfalls was compiled for the road N-634 connecting Zarautz and Getaria, based on highway administration data and press sources. According to the recorded historical events, six (from A to F) volume ranges were considered (Table 2). For the sections of the road N-634 (5 out of 20) , the frequency was then assessed as the number of events divided by the number of observation years.

Figure 3: Examples of rockfall magnitudes (C, D, E, and F) in the study area, in relation to the classes of Table 2 (source: photo D, E: Javi Colmenero; F: Servicio Geológico de Obras Públicas)

Table 2: Magnitude classes and respective annual frequency for the road N-634 connecting Zarautz and Getaria.

Class	Volume (m^3)	# events	Period	Time span (years)	events/yr
A	<1	104	1994-2009	15	6.933
B	1-5	91	1994-2009	15	6.067
C	5-50	24	1994-2009	15	1.600
D	50-500	5	1960-2009	49	0.102
E	500-5,000	1	1884-2009	125	0.008
F	>5,000	1		>330	<0.003

Although the same amount of information is not available for all the PoR, numerous in situ inspections at the PoR have provided extensive topographical and geological data, which can be used for estimating the frequency at the rest of the sections. To this aim, a geomorphological description was made for 18 representative examples with known frequency of events, on the road N-634. Then, for the rest of the sections with no frequency data, the same frequency values were established, for the sections within the same geomorphological class. The main assumption is the equivalence of the frequency at slopes with similar geo-structural characteristics, number of recent scars, slope height and block size. The suggested indicators to characterize geomorphologically the slope are the joint persistence (I_P), the scar density (I_{DC}), differential erosion (I_E), the number of potentially unstable rock masses (I_{FP}), and the Slope Mass Rating Index (I_{SMR}). These indicators are calculated as follows:

- The persistence of discontinuities in the rock mass, I_P, is assumed high when planes of several tens of meters can be observed on the slope face; moderate when of some meters; and low when it is sub-metric. The stratification is taken into consideration as well. Higher persistence of discontinuities results in the existence of more planes permitting the block detachment from the slope face.

- The scar density, I_{DC}, is calculated as the ratio of the number of recent scars to the slope height. Scars can be noticed as areas with a different colour (often reddish) from the rest of the slope face. Greater number of recent scars indicates higher and more frequent activity.
- Differential erosion, I_E, can be present or absent and can be observed at rock masses constituted by materials of distinctive strength. Differential erosion leads to loss of support for the overlying rock mass.
- The number of potential rockfalls, I_{FP}, refers to the number of potentially unstable rock masses as observed by in situ inspections. This number is collected distinguishing between magnitude classes.
- The Index Slope Mass Rating I_{SMR} is the value of SMR, as proposed by Romana (1991).

Table 3: Scoring of the geomorphological indicators used for the rockfall frequency assessment.

Scores	0	1	2
Indicators			
I_P (Joint persistence)	Low	Moderate	High
I_{DC} (Density scars)	<0.1	0.1-0.3	>0.3
I_E (Differential Erosion)	No	Yes	(Not applicable)
I_{FP}(Number of points with potential rockfalls)	<2	3-10	>11
I_{SMR} (SMR)	>80	40-80	0-40

Each indicator, depending on its value, scores 0, 1 or 2 points, applying the criteria of Table 3, with the exception of I_E, which scores up to 1. The indicator scores are summed up to provide the frequency index I_F according to Eq. (2). We established the thresholds to relate the geomorphogically-based index I_F with the frequency of the events, after application to the sections with known frequency, as shown in Table 4.

$$I_F = I_P + I_{DC} + I_E + I_{FP} + I_{SMR} \,, \tag{2}$$

Table 4: Annual frequency f_a for different I_F values.

I_F	Annual frequency f_a (events/yr)
8-9	≥3
6-8	$1 \le f_a \le 2$
5-6	$0.2 \le f_a \le 1$
3-5	$0.1 < f_a \le 0.2$
0-3	≤0.1

During the in-situ inspections data is collected for the relative frequency (%) of potential rockfalls per volume class, and for the most frequently encountered rockfall size on the slope (modal). The annual number of events per volume class is calculated by multiplying the total annual frequency with the relative frequency of each class. If the relative frequency data has not been collected, risk calculations are made for the modal size, as an average approximation.

The implementation of stabilization measures (bolts, anchors), retention (nets and/or gunite), or protection (barriers, galleries), partially or entirely, reduces the annual frequency of rock blocks reaching the roadway. To account for this, a corrected reduced frequency F_{rc} is proposed to be used, upon a correction factor n (Table 5), according to Eq. (3):

$$F_{rc} = \frac{F_r}{10^n} \ , \qquad (3)$$

where,

F_{rc}: annual corrected frequency

F_r : annual frequency before correction

N: correction factor given by Table 5.

Table 5: Correction factor for different protection measures, to be applied on the annual frequency according to Eq. (3), for each magnitude.

Magnitude (m^3)	**A**	**B**	**C**	**D**	**E**	**F**
Volume (m^3**)**	<1	1-5	5-50	50-500	500-5,000	>5,000
Gunite, bolts (effective and extense)	0.5	0.25	0	0	0	0
Gunite, bolts (partial)	0.25	0.1	0	0	0	0
Shotcrete with bolts	1	0.5	0	0	0	0
Cable nets	0.25	0	0	0	0	0
Triple torsion nets	0.5	0	0	0	0	0
Low rigid foot barrier	0.25	0	0	0	0	0
High rigid foot barrier	1	0.5	0	0	0	0
High rigid foot barrier (partial)	1	0.5	0	0	0	0
Ditch width <5 m	0.2	0	0	0	0	0
Ditch width <5 m with vegetation	0.5	0.1	0	0	0	0
Ditch width >10 m	0.5	0.25	0	0	0	0
Ditch width > 15 m	1.5	1	0	0	0	0
Flexible Barriers <2000KJ	3	1	0	0	0	0
Flexible Barriers >2000KJ	3	2	1	0	0	0
Gallery	4	3.5	3	2	1	0

The thresholds of Table 3 for the scoring of indicator, the I_F values and the annual frequency as indicated in Table 4, were obtained after a trial and error iterative procedure, so as to optimize the matching of the results with the observed frequency from real events at natural slopes (the latter marked as 1-2 events per year, or 1 event every 1-5 years, or 1 event every 5-10 years). The results from this iterative procedure yield an overestimation of maximum 2 events per year in 5 sections, while at the rest of the sections the results are compatible. At a second stage, further calibration was performed considering the protection measures, which yields the correction factors of Table 5.

The risk at each point is then calculated for each PoR by the general Eq. (1). For this, the consequences are assessed per rockfall magnitude class as indicated in Table 13 of the Appendix. The six magnitude classes, also shown in Table 2, were defined judgmentally, based on the principal consequences and disruption of the road, as observed from previous rockfalls and road maintenance interventions. In Table 13 the principal consequences and disruptions are shown for each magnitude class, as the respective actions which are used as a guide for the establishment of the costs in terms of UC.

3.2 Failure of retaining structures (RS)

Another objective of this work was the analysis of the risk related to the failure of anchored reinforced concrete walls. The uncertainties characterizing the structural design parameters and the terrain resistance are substantial, thus the safety level of these structures cannot be precisely assessed. The probability of failure is considered instead.

The hazard level associated to the anchored retaining walls is evaluated on the basis of a hazard index, HI. The evaluation consists in a modification of the Methodology for the Revision of Anchors, developed by the company Euroestudios in 2004. According to it, the HI for the retaining structures is equal to the average of the scores assigned to three components (Eq. 5). These components and their scores are presented in Table 6 and they are: the safety factor of the wall, the anchorage design (DA), and the project and construction quality (PQ). The scoring for each component ranges between 1 and 5. Moreover, to calculate the scoring of the index DA, the average value from 3 parameters is considered according to Eq. (4): % working load/ultimate load ratio (UL), grout length per ten tons load (GL), and the anchoring ground (AG). The term sound rock or mixture refers to the ground where the structure is anchored. For the parameter PQ there are three possible scores: 1, if “Available data for anchors” is yes and “Technical assistance during construction” is yes; 3, if “Available data for anchors” is no and “Technical assistance during construction” is yes; and 5, if available data for anchors” is no and “Technical assistance during construction” is no.

Table 6: Scores the hazard index HI components, for the failure of retaining walls.

Parameter		Value				
		1	2	3	4	5
Safety Factor (SF)		>2	1.55-2.0	1.45-1.55	1.30-1.45	<1.30
Anchor Design (DA)	Working load (% Ultimate load) UL	<55		55-65		>65
	Grout Length GL	>1.2m/10t		0.8-1.2m/10t		<0.8m/10t
	Anchoring ground AG	Sound Rock		Mixture		Weathered soil/rock
Project and construction (PQ)	Available data for anchors	yes		no		no
	Technical assistance during construction	yes		yes		no

The hazard index (HI) is obtained using the following Eq. (4) and (5):

$$DA = \frac{UL+GL+AG}{3}, \qquad (4)$$

$$HI = \frac{SF+DA+PQ}{3}, \qquad (5)$$

The thresholds and the scoring of the parameters were established based on expert judgement, increasing the hazard index when the function of the anchors is critical or uncertain, and decreasing it when loading conditions and supports, as well as when good practices in construction can guarantee a good function of it. In Equations (4) and (5), for simplicity, all factors are equally weighted.

Silva et al. (2008) have associated the safety of factor of engineered slopes, for a given project category, with the probability of failure. For this, the structures are classified according to the level of engineering design. Category I comprises engineered slope which were designed, constructed and managed using the most advanced state of the art knowledge. Category II includes constructions with normal standards. Category III are constructions without specific design that do not follow standards, and Category IV those ones with a poor or completely missing engineering knowledge basis. As the HI is an adaptation of the SF that takes into consideration additional criteria for the level of functioning of the structure, a similar relation between annual probability of failure of the anchored retaining walls can be established as well. The relation is presented in Fig. 4 and Table 7.

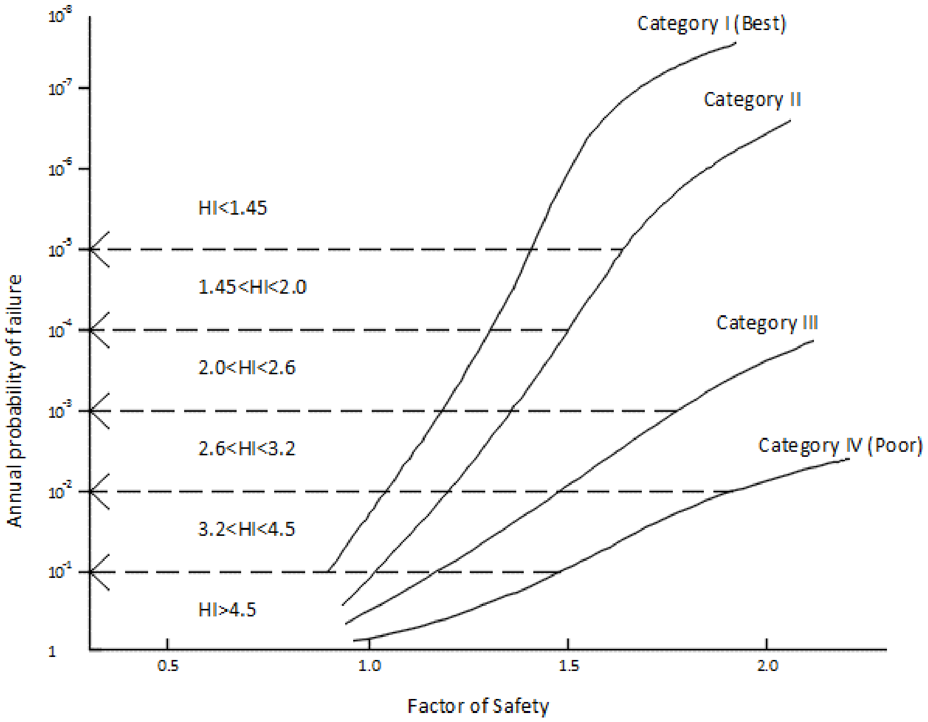

Figure 4: Classification of the engineered slopes and relation to the annual probability of failure (modified from Silva et al. 2008).

Table 7: Annual probability of failure for HI values, according to Fig. 4.

Annual probability of failure (Pr)	Hazard Index (HI)
$0.1<P$	$HI > 4.5$
$0.01<P\leq 0.1$	$3.2<HI\leq 4.5$
$0.001\leq P\leq 0.01$	$2.6<HI\leq 3.2$
$0.0001\leq P\leq 0.001$	$2.0<HI\leq 2.6$
$0.00001\leq P\leq 0.0001$	$1.45<HI\leq 2.0$
$P\leq 0.00001$	$HI\leq 1.45$

The proper design and construction of the anchored retaining walls should be reflected in the absence of deformations and anchor overloading. Increased pressure at the load cells, deformations, cracks and wall tilting are interpreted as instability indicators. In that case the annual probability of failure P_r should be increased. Thus, factors of increase are added to the initial value of the HI, as shown in Table 8. The availability of this information implies that periodic and detailed wall inspections are carried out.

Table 8: Increase factor of the HI according to instability indicators at the retaining walls.

HI Increase	Increase of the service load	Deformation of the retaining wall and or/terrain
1	Pressure increase of <65% of ultimate load	Deformation <3mm/a

	External factors (groundwater table changes, erosion…)	Cumulative deformation >30% of the maximum allowable deformation of the concrete
2	Pressure increase of >65% of ultimate load	Deformation >3mm/a
		Cumulative deformation >60% of the maximum allowable deformation of the concrete
		Presence of cracks, tilting, etc
		Non instrumented retaining wall

For measuring the consequences, we distinguished between the failure of small retaining walls, retaining walls shorter than 6m, and higher than 6m (Table 13-Appendix). The length of the affected road section, considering the spreading of the debris, was empirically fixed as the triple of the wall height at the section.

3.3 Slow moving landslides (SL)

The involved landslides at the PoR have a persistent creeping movement, which in a worst-case scenario can lead to a sudden acceleration. The clay materials in the study area have a viscous behaviour, characterized by resistance increase as the movement rate increases. High rainfall precipitations often result in landslide reactivation, with centimetre displacements. As this analysis involves active landslides or landslides with episodic reactivations, the challenge here was to assess the probability of a given damage level, in function of the landslide movement rate. All the road sections analysed here, lay on previously and well identified landslides, and as such movements are associated with landslide activity.

Mansour et al. (2011) indicated that a relation may be established between the damage expected from slow-moving slides to roads, versus the displacement rate. They proposed ranges for the annual displacement rate leading to different extents of damage, which are 0-10, 10-100, 100-160, 160-1,600, and >1,600 mm/year corresponding to limited, minor, moderate, severe damage or total road destruction, respectively. They also provided a description for each damage extent with respect to the type and frequency of the actions to be taken, for its repair. The aforementioned ranges do not distinguish between horizontal and vertical deformations, on one hand, and on the other, they are based on the assumption that continuous and almost constant movement takes place.

Instead, our experience in Gipuzkoa shows that landslide reactivation is episodic and can be sudden, producing deformations even in short periods, such as few days or weeks. Although those deformations are usually of centrimetric order, they can cause cracks, bumps and puddles on the pavement, and jeopardize road traffic safety. For this reason, more restrictive criteria that those proposed by Mansour et al. (2011) were applied. They relate the maximum observed horizontal landslide velocity and the annual horizontal displacement rate to the annual probability of exceeding a damage level. The following paragraphs describe how they were established.

In the case study, horizontal velocity data is available from the inclinometer measurements. After 2010, deformation readings have been constantly taken, every 3 months. In that sense, although the monthly velocity measurements have a limited precision, they can provide certain information on the landslide movement patterns. We inspected the in-situ damage, in order to establish the relation between the velocity and the road damage. Four levels were identified, as shown in Fig. 5 and described qualitatively in the following:

- Damage level A (landslides of low intensity): There are rarely cracks and deformations. No speed reduction is required while driving. Crack sealing and resurfacing is periodically performed for periods longer than 1 year.
- Damage level B (landslides of moderate intensity): Damage includes pavement deformation and cracks and/or roadside destruction, without affecting the functioning of the road. If proper signalling is present, the chance of an accident is very low. Traffic conditions can be normally maintained if regular sealing and resurfacing is performed, until a more permanent solution.
- Damage level C (landslides of high intensity): Pavement deformation is substantial, including the presence of steps and puddles, and partial rupture of the platform affecting partly or entirely traffic lanes and/or the roadside. The normal functioning of the road is disturbed. Traffic is not interrupted, although restrictions such as alternative pass and traffic lights regulation are required. Accidents might occur if the vehicles enter the affected zone, without previous signalization. The normalization of the traffic conditions requires slope stabilization and road repair.
- Damage level D (landslides of very high intensity): Displacements are of the same order of magnitude as for level C, however with the vertical component prevailing and giving place to complete destruction and loss of the pavement continuity. This situation is typical for roads situated on the crest or on the boundaries of landslides. The functioning of the road is seriously affected. There is a high likelihood of an accident due to vehicles falling into the generated depressions. Important stabilization works and reconstruction of the road are required.

Figure 5: The four damage levels identified at the roads of Gipuzkoa: (top-left) No/Slight damage, (top-right) Moderate damage, (down-left) Severe damage, and (down-right) Partial/total destruction.

To establish damage proxies for the calculation of the expected consequences we correlated the observed road damage with the indications of the inclinometers at 24 reference PoR. The correlation was found to be positive, as, in most cases, increasing displacements were associated with more severe damage. In particular, the maximum horizontal monthly velocity and the cumulative displacement were used as the two proxies for the damage. For the establishment of the thresholds that relate the damage level with the terrain displacements, we tried to maximize the right predictions (when the observed damage level is the same with the calculated damage level), and at the same time to achieve a balance between damage underestimation and overestimation. The proposed thresholds are summarized in Table 9. Out of the 24 PoR, 20 yield right predictions, 1 presents damage overestimation and 3 damage underestimation (out of which, the measurements of 1 inclinometer are not reliable). Partial/total destruction occurs when the criteria for severe damage plus either one of two further criteria are fulfilled: the road is located inside the landslide scarp or a shear crack has being formed (the scarp manifests itself in semi-circular form on the pavement).

Table 9: Damage criteria in function of landslide velocity (MHDR: maximum monthly horizontal displacement rate; ACDR: annual cumulative horizontal displacement).

Damage levels	MHDR (mm/month)	ACDR (mm/a)	Landslide intensity	Further criteria
A: No / slight damage	<3	<30	low	
B: Moderate damage	3-10	30-100	moderate	
C: Severe damage	>10	>100	high	
D: Partial/total destruction	>10	>100	very high	Road inside landslide scarp and/or shear crack

For the slow moving landslides, the hazard was expressed in terms of temporal probability of reactivation with an intensity exceeding a given level of damage. To assess the temporal probability we first distinguished between the landslides that are responsive to intense rainfall precipitations, from those for which a clear relation between rainfall and reactivation cannot be established. For each case, typical movement patterns were observed from the inclinometer measurements. Four patterns were identified depending on the maximum monthly velocities. For each type (responsive and not responsive) and each pattern O, X, Y or Z as described in the following, the probability of reactivation with an intensity leading to low (A), moderate (B) and high (C) or very high (D) damage is determined.

As most landslides in the study area are creeping, undergoing continuous small deformations, the probability of low damage is always high (P∼1). For some of them, acceleration takes place for intense or long rainfall periods. Moderate, high or very high damage might then occur with an annual probability equal or lower than 1. The assessment of the probability is herein based on the return period of two major extreme rainfall events in the area.

The two extreme events were recorded during the observation period covered by the monitoring network of the Gipuzkoa Road Authority and they are: (1) the rainfall events of 4 to 7 November 2011 that were of high intensity and short duration. The rain recorded at the Añarbe Dam on the 6th of November 2011 was 185 mm, which according to the Water Management Agency of the Basque Country, corresponds to a return period of the order of 100 years; (2) the rainy period of January-February 2013 that was characterized by moderate to low daily intensity but of long duration, with cumulative precipitation measurements that exceeded the maximums of the reference period 1971-2000, and a return period of over 100 years according the Euskalmet (Basque Meteorological Agency).

Accordingly, it can be assumed that the annual probability of reactivation or sudden acceleration of the instrumented landslides that have not experienced deformations during the two afore-mentioned events is lower than $\mathrm{P} = 0.01$ $(\sim \frac{1}{100})$. Using this probability as a reference, the reactivation probability for the different patterns and types is defined empirically, according to the observed number of peak month velocities on the inclinometer measurements.

For slow moving landslides which are responsive to rainfall events, we distinguish between four movement patterns (Fig. 6).

- Pattern O: Landslides which are inactive or extremely slow, which have not experienced deformations neither in extreme nor in common precipitation conditions. The annual probability of reactivation is P=0.01.
- Pattern X : Landslides with a high probability of reactivation and low intensity, characterized by displacement rates lower than 2-3 mm/month and cumulative displacements lower than 30 mm (Fig. 6, top-left). They have not experienced significant accelerations for the two afore-mentioned extreme events. Low damage A is mostly expected.
- Pattern Y: Landslides with a high probability of reactivation and low/moderate intensity, characterized by displacement rates mostly lower than 5 mm/month and cumulative displacements 30-100 mm (Fig. 6, middle-left). They have experienced some accelerations for the two extreme events, with a displacement rate under 10 mm/month. Low or moderate damage (A or B) is mostly expected.
- Pattern Z: Landslides with a high probability of reactivation and moderate/high intensity, characterized by rates higher than 2-3 mm/month and cumulative displacements greater than 100 mm (Fig. 6, bottom-left). They have experienced accelerations for the two extreme events, exceeding the displacement rate of 10 mm/month. For the PoR where the road is situated on the crest, we consider that they follow the pattern Z, irrespectively of the inclinometer measurements. High or very damage (C or D) is mostly expected.

Using the intensity-damage correlations of Table 9, the annual probabilities of exceedance of a given damage level were established, as shown in Table 10. Similar patterns were detected too for landslides which are hardly or not at all responsive to rainfall events (Fig. 6, right column), even for the two afore-mentioned extreme events. In that case, higher probability values are set in order to reflect the increased uncertainty for the causes leading to the terrain acceleration (Table 10).

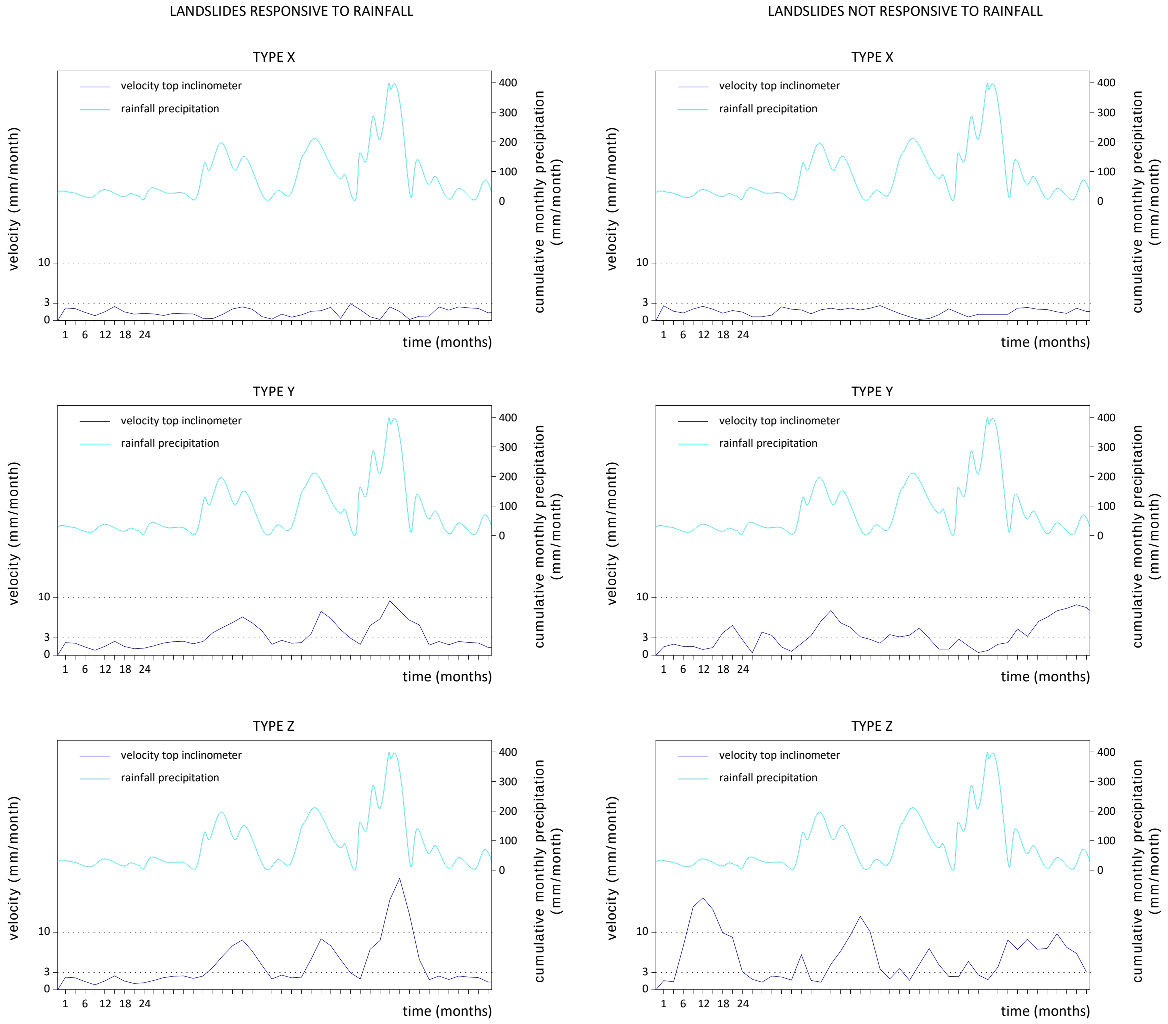

Figure 6: Patterns of movement for landslides responsive (left) and not responsive (right) to rainfall.

Table 10: Annual probability of exceedance of a damage level and (in parenthesis) return period in years.

	Intensity	Type O	Type X	Type Y	Type Z
Responsive to rainfall	Low (P_l)	0.01 (100)	1 (1)	1 (1)	1 (1)
	Moderate (P_m)	0.01 (100)	0.02 (50)	0.5 (2)	1 (1)
	High (P_h)	0.01 (100)	0.002 (500)	0.01 (100)	0.02 (50)
	Very high (P_{vh})	0.01 (100)	0.002 (500)	0.01 (100)	0.02 (50)
Not responsive to rainfall	Low (P_l)	0.01 (100)	1 (1)	1 (1)	1 (1)
	Moderate (P_m)	0.01 (100)	0.05 (20)	1 (1)	1 (1)
	High (P_h)	0.01 (100)	0.005 (200)	0.02 (50)	0.05 (20)
	Very high (P_{vh})	0.01 (100)	0.005 (200)	0.02 (50)	0.05 (20)

The consequences, actions and costs related to slow-moving landslide damage repair that were used for the risk assessment and for the characteristics of the case-study are also reported in Table 13 (Appendix). The risk calculation for slow moving landslide is also based on the general Eq. (1). Nevertheless, in this case, for the realistic application of that equation three further points should be taken into consideration:

1) The probabilities of high or very high damage alternate when applying Eq. (1), depending on the location of the road section on the body (high damage) or on the scarp of the landslide (very high damage), and/or the absence (high damage) of presence (very high damage) of a shear crack on the road platform.

2) To calculate the total expected cost, the UC of Table 13 has to be multiplied with the affected road section length (multiples of 10 m), for all damage levels. The affected section length is expected to vary for each damage level, in different percentages of the (total) road length that is marked between the landslide boundaries. For no/slight damage the percentage 10% of the total road length is taken, for moderate damage 20%, for severe damage 50%, and for partial/total destruction 100% (worst case scenario).

The reasons for reducing the affected road section to a percentage of the total road section in the landslide are the following:

i) Some of the landslides in the study area demonstrate composite and complex movements, incorporating multiple smaller sliding bodies, with very local displacements. In that case, instabilities and reactivations take place only locally, affecting only smaller fractions of the road;

ii) The landslide velocity is expected to present variations within the landslide body. More severe damage often demonstrates only at limited sections of the road, corresponding to the local highest movement rates. This might occur mostly for lower velocities, while higher velocities are more probably related with a generalized instability and damage.

iii) Minor displacements can be accommodated by the pavement (especially for flexible pavements), thus they do not result in damage of the entire road section. Major displacements, instead, result in greater stresses and strains for the pavement and more extensive damage, especially for rigid pavements that cannot accommodate them.

3) In the case of slow-moving landslides, the annual probabilities for the different damage levels should be mutually excluding, for the risk calculation. The values of Table 10 provide the annual probability of exceeding a given damage level. Thus the annual probability of damage A, P_A, (none/slight) is the annual probability of exceeding damage A minus the probability of exceeding damage B (moderate). Accordingly, the annual probability of damage B, P_B, is the annual probability of exceeding damage B minus the probability of exceeding damage C or D (partial/total destruction or severe damage). The annual probability of damage C or D, P_C or P_D , is equal to the annual probability of exceeding damage C or D. All probabilities should be in the range [0,1], thus if the result from the above calculations is negative, P_A, P_B, P_C and P_D are taken as 0.

After incorporating these modifications, Eq. (1) is modified to Eq. (6) for slow moving landslides.

$$\mathrm{R_{SL}} = \mathrm{P_l} * 0.1 * \mathrm{L} * \mathrm{C}_l + \mathrm{P_m} * 0.5 * \mathrm{L} * \mathrm{C}_m \quad + \mathrm{P_{h(or\,vh)}} * 1.0 * \mathrm{L} * \mathrm{C_{h\,(or\,vh)}} \quad , \tag{6}$$

Where:

R_{SL}: Risk for slow moving landslide

Pj: Annual probability of a given damage level (j takes the value of l:low, m:moderate, h: high, and vh: very high)

C_j: Consequences corresponding to the velocity associated with the given damage level, in terms of UC

L: total length the affected road section (multiples of 10 m).

4. Application examples and results

The methodology is being applied on a periodic basis to the road network of Gipuzkoa. The calculation of the risk for the different hazards was organised using automatized Excel data sheets, where the user introduced the required data from a closed list of options. Some application examples for selected PoR are presented here. The overall results for all analysed PoR during the 2015 inspection are shown in section 4.4. Due to space limitations, only the most important data needed for the application of the proposed methodology are provided here. An extended archive with further details on the location and type of instabilities, accompanied by images and maps and detailed descriptions have been at the disposal of the authors. For the same reason only a limited number of figures presenting the current state of the road have been included too.

4.1 Rockfalls

We indicatively present the risk for two different cases of rockfall affected sections: the PoR L1C, situated at the local road GI-3324 (from km 0.700 to 1.450) and the PoR P4C of the highway N-1 (km 407.395 to 407.680). The two PoR are shown in Fig. 7.

Rock instabilities at the PoR L1C are due to the unfavourable structural conditions of the rock mass, leading to planar and wedge failures, with a safety factor of the blocks on the slope seemingly smaller than 1. In some few areas toppling mechanisms are also observed. Although rockfalls occur with a frequency higher than 2 events per year, there is no historical record of the events. The road platform is in a good state without major impact signs, indicating that no high magnitude events have been occurring. Thus, the magnitude-frequency relation of events here is evaluated considering the slope properties from Table 3, and applying Eq. (2) for the calculation of the I_F. For I_P (joint persistence): Low, I_{DC} (density scars)>0.3, I_E (differential erosion): Yes, I_{FP} (number of points with potential rockfalls)>11, and I_{SMR} (SMR index): 40-80, I_F results to be 6, which corresponds to an annual frequency of events equal to 1 (from Table 4). This frequency is proportionally distributed amongst the magnitude classes A, B and C, according to the in situ observed relative frequency of potential unstable volumes (45% for <A: 0.5m^3, 40% for B: 0.5-5 m^3, 15% for C: 5-50 m^3). This results in annualized expected frequency of events equal to 0.45, 0.40 and 0.15, respectively for each magnitude class. No protection measures exist, thus no correction is made on that frequency. The risk is then calculated for each magnitude size A, B and C and summed up after Eq. (1), considering the UC, of Table 13. The total annual risk for L1C is 1.55.

For the PoR P4C, a similar procedure was followed. For I_P: Moderate, I_{DC} >0.16, I_E: No, I_{FP}: 4, and I_{SMR}: 0-40, I_F results equal to 5, which corresponds to an annual frequency of events equal to 0.2. This frequency is distributed to the magnitude classes: 0.08 for A, 0.09 for B, 0.01 for C, 0.01 for D and 0.01 for E. In this case, a correction is applied on the annual frequency. Considering that the slope is partially protected by gunite and bolts in a bad state of maintenance, and that a ditch with width smaller than 5 m exists, the summative frequency correction factors for the two types of measures from Table 6 are 0.45 and 0.2 for magnitudes A and B. For higher magnitudes, the existing protection measures are not considered to be efficient. The annual frequencies per size after correction are 0.03, 0.07, 0.01, 0.01, 0.01 for A, B, C, D and E, respectively, which after multiplication with the correspondent

UC and summing, they result in a higher total annual risk than the previous one, and equal to 3.05. The higher risk is ought to the existence of bigger rock blocks which cannot be retained by the actual protection measures.

Figure 7: (left) PoR L1C of the road GI-3324 (from km 0.700 to 1.450), without protection measures; (right) PoR P4C of the road N-1 (km 407.395 to 407.680) with protection measures.

4.2 Anchored retaining structures

Two further examples, for the risk related to the failure of anchored retaining structures are presented (Fig. 8).

The first one is the highway section P2A, where two anchored walls sustain a weathered flysch rock mass. The two walls cover the upper and middle part of the slope. The upper wall has a length of 60 m, with 24 anchors and the lower is 42 m long with 42 anchors. The slope has an inclination of 35 degrees in the first 20 m and of 20 degrees in the rest of its length. At the bottom of the slope there is a concrete wall. During the construction works of the N-121-A, water seepage was detected on the middle and upper parts of the slope, which have been related to the mobilization of soil. The slope is monitored with inclinometers, piezometers and the walls with hydraulic load cells, given the existence of an urbanized area on the top of it. In the upper part of the slope there a weathered zone, with an estimated thickness of 20 to 22 m, which determined the type and length of the anchors.

Following the procedure described in section 3.2, for a Safety Factor >2 (1 point from Table 6), working load <55% (1 point), grout length >1.2 m/10 t (1 point), anchoring ground is a mixture of sound and weathered rock (3 points), available data for anchors and technical assistance during construction (1 point), the calculated hazard index from Eq. (5) before correction is 1.222. Given the presence of cracks in the lower wall, a correction factor of 2 is applied to the HI, which becomes 3.222 and the corrected annual probability of failure is then 0.0072 (from Table 7). The upper and lower walls together have a total height of 8 m. When applying the general risk equation the respective costs from Table 13 are considered and adjusted to the total length of the affected road section (24 m or 2.4 x 10 m), and they are found to be 290.4 UC. The total risk for this section, as the product of failure probability with that cost is equal to 2.09.

The second section, the PoR C8A corresponds to a rocky slope of 240 m and height 37m, of an average inclination of 45 degrees. It is treated with gunite with a protection net and a reinforcement of 646 bolts of 16 m length. The works for the reinforcement of this slope were performed between 1992 and 1993, with 8 strips of gunite, 5 m tall each one. Every strip includes 4 rows of bolts, except the lowest one which has 5 rows and the crest which does not have any. The load cells indicate that presently several bolts are overloaded. The rock mass is slightly to moderately weathered over the entire slope. The maximum volume that has been estimated to be unstable is 21,800 m^3.

The parameters that have been used for the C8A are (Fig. 7, right): Safety Factor <1.30 (it is not known for this case) (5 points), working load >65% of the ultimate load (5 points), grout length >1.2m/10 t (1 point) and anchorage on a slight to moderate weathered rock (3 points). Although data exists for some anchors, it is not available for all of them, which is penalized assuming the respective value of “no” in Table 6. Construction was performed with technical assistance. The initially calculated HI is 3.67. As the bolt pressure increase is greater than 65% of the ultimate load (up to 80%), the HI is increased by 2 and it is 5.667 which corresponds to an estimated failure probability of 0.82. This value was calculated according to Table 7, after fitting a power law curve to the HI and the probability threshold values mentioned therein. As the wall height is H > 6 m and the affected road length is 111 m the total cost is 1343.1 UC and the risk is 1,101.34, which is substantially higher than the previous one, as a consequence of the higher hazard in this section.

Figure 8: (left) PoR P2A of the road AP-8-1-1 (from km 77.140 to 77.210) where the crest of the slope and the retaining wall with anchors is seen; (right) C8A of the road G-2634 (32.980 to 33.150) with gunite, rock bolts, and anchors.

4.3 Slow moving landslides

Two examples of PoR, subjected to damage for being situated within slow moving landslide areas are presented here: the C3C and the C9G (Fig. 9).

The PoR C3C involves a rotational landslide, occurring in the interface between clay colluvial soil and rock. It affects a road section of almost 200 m, with a retaining wall of 1 m height, along 41 m. There is not a historical record of the damage evolution. The road platform is found to be cracked and vertically deformed, as well as the ditch. For about 20 m the cracks are 2-3 cm open and mostly affect one direction of the road. The most probable reason for the instability is the presence of water and the deficient drainage causing humidity and water flows.

Slope movements occur during high rainfall episodes, which was also confirmed by the indications of the inclinometers as explained in the following.

There are two inclinometers that started measuring since November 2013, initially with monthly frequency, which are 14.5 and 15.5 m deep each. Movements were found to be concentrated at a depth of 0.5-2.0 m (corresponding to the thickness of the colluvium soil layer). The inclinometer measurements indicate that the soil movements directly respond to the total monthly precipitation intensity, expressed in mm/month, with records of up to 8 mm/month and cumulative displacement higher than 100 mm. These movement rates correspond to Pattern Z (Fig. 6, left). According to Table 10, the annual probability of exceeding low damage is 1, of moderate damage is 1 too, and of high damage is 0.02. As field inspections indicated that no scarp or shear crack are present, the potential of very high damage was eliminated. Consequently, the probability of occurrence of only high damage is P_h=0.02, of only moderate damage is P_m=1-0.02=0.98, and of only low damage is 0 (moderate damage constantly overlaps with low damage). Applying Eq. (2) and the costs of Table 13 for a total length of affected road of 200 m, the risk result here is 66.18.

The soil instability affecting the C9G is ought as well to colluvial soil accumulations of 3-4 meters depth, over the bedrock. There are visible settlements and the ditches are deformed. The landslide is instrumented with two inclinometers that indicate that it is active.

The inclinometer measurements indicate vertical displacements lower than 2-3 mm and cumulative displacement lower than 30 mm, which points to a movement pattern of type X. There is not any scarp or developed shear displacements. Accordingly the probability of exceeding low damage is 1, moderate damage is 0.05 and high damage is 0.005. As previously, the probability is calculated for high damage: 0.005, for moderate damage: 0.045, and for low damage: 0.5, which for total a length of 300 m, and the same as previously costs, gives a total risk of 10.84.

Figure 9: Road sections situated within slow moving landslides, with damage: (left) PoR C3C of the road GI-2133 (from km 8.280) with observed deformations and cracks on the road pavement; (right) PoR C9G of the road GI2637 (from km 17.891 to 18.220) showing minor cracks already sealed.

4.4 Overall results and discussion

As aforementioned in section 2, out of the totally 84 PoR, 20 concern rockfalls, 37 anchored walls, and 27 slow moving landslides. The classification of the risk was based on economic criteria, considering that it expresses the average annual repair cost at a section. Four risk levels were used: low (<1 UC), moderate (1-10 UC), high (10-100 UC), and very high (>100 UC).

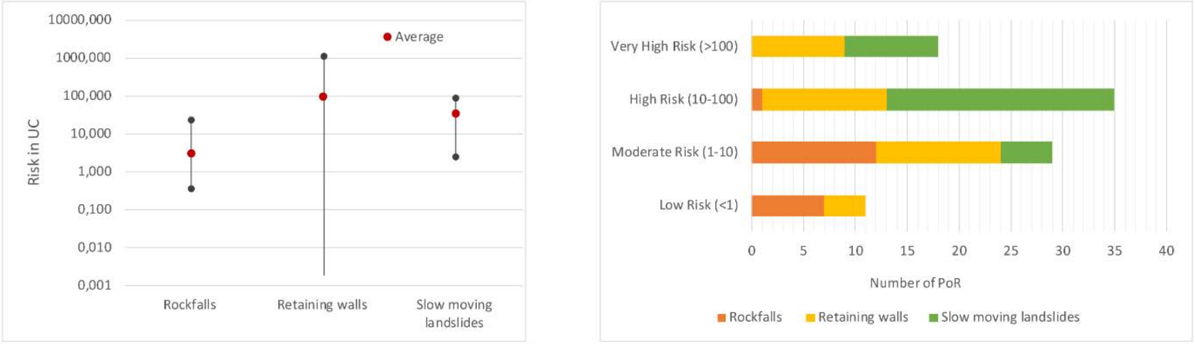

Figure 10: (left) Average, maximum and minimum calculated risk for each hazard type; (right) Number of PoR per hazard type in each risk class.

Figure 10 shows how the risk levels are distributed over the different hazard types. High risk areas mostly involve retaining wall failures or slow moving landslides. Rockfalls principally cause low and moderate risk. The risk classification highlights 21% (18 PoR) of the analysed sections being of very high risk and needing imminent protection interventions. The highest risks in the study site (above 100 UC) were observed for 9 of the retaining structures. 42% of the PoR fall into the class of high risk, 35% of moderate risk and 13% of low risk. Depending on the prioritization needs and the economical restrictions for the planning of the interventions, other thresholds can be used for the risk classification, in order to reduce the number of sections marked as of highest priority.

The risks corresponding to the repairs related to the failure of the retaining walls can be one order of magnitude higher than for the rest of the hazards. This is reasonable given the fact that, besides road cleaning and repair costs, the additional wall construction/repair costs are high and that for this type of events, high soil masses can be mobilized.

The calculated risks overestimate the real average annual costs, as they do not take into consideration that after protection interventions, the hazard is reduced and the chances of damage for the following period are much lower. Moreover, in practice, low and moderate damage is not repaired each time it occurs, even if required, but in larger time intervals, which reduces the real repair costs.

The values calculated here for the risk components are not precise but carry a certain degree of uncertainty as also in other quantitative landslide risk studies (Jaiwsal et al. 2010, Vega et al. 2016, Corominas et al. 2014). An extensive quantification of the uncertainties and their effect on risk calculation procedure is a challenging task, and has not been included here. However, some principal sources of uncertainty are mentioned in the following, with the aim to highlight steps in the procedure which present high degree of uncertainty and might have a strong effect on the final risk results.

For rockfalls, it is the attribution of large frequency values to the high magnitude classes E and F, that results in excessive costs. In any case, the definition of a maximum rockfall volume in a slope is a complicated issue, especially considering the structural geology and the existence of bridges in the rock mass with a given persistence (Corominas et al. 2018). The mobilised volume for the failure of anchored retaining walls also implies a high degree of uncertainty with a substantial effect on the final risk. When it comes to slow moving landslides, where the frequency and intensity assessment is based on the inclinometer measurements, uncertainties are associated with the location of the inclinometers in the landslide, the frequency of the measurements that also determine the precision of the velocity values, the potential existence of deeper rupture surfaces with displacements which are not registered by the actual inclinometers, and operability issues too. Through the entire procedure, the definition of different thresholds presents moderate uncertainty as these were selected to fit the best real event occurrences, with a certain coherence, as explained, respectively for each hazard, in the previous sections. The same for the association of magnitude and intensity of events with damage, as the actions acting on the road and causing its damage are complex and the roads also vary in size, materials and resistance.

The occurrence of landslides in areas intersecting transportation corridors might affect societies and the built environment in an extensive way (Remondo, 2008). The related indirect risk involves the impact on lifeline systems (e.g. water and sewage system, energy and lines of communication) in the vicinity of the roads, and present in the path of landslides. Interruption of access to and from rural and urban areas and critical transportation infrastructure like airports, ports, and bridges, as well as other medical, educational, industrial and other critical facilities, may cause important social and economic loss. Touristic, commercial, business activities, as well as real estate values are amongst the most commonly affected. Given the multiple dimensions and cascade effects that are inherent in such situations, indirect risks might entail large scale consequences, which, in monetary terms, substantially exceed the direct risks. The establishment of the links and intersections, leading from the initial hazardous process to (some of) the afore-mentioned consequences presents certain perplexity, the investigation of which is out of the scope of this work. Simplified procedures as the one presented by Corominas and Mavrouli (2015) have been proposed in the past for the study area. Despite this, the work presented here is limited to the investigation of the risk related to the direct losses, and does not take indirect losses into consideration.

5. Conclusions

In this paper a procedure for the quantification of risk related to the geotechnical hazards across a road network has been presented. The studied hazards are rockfalls, failure of retaining structures, and slow moving landslides. The risk has been calculated in monetary terms, as multiples of a Cost of Unit set at 1000 €.

In the studied area, the extensive and periodic collection of data permitted the magnitude-frequency evaluation based on historical data and, for rockfalls, where this data lacked, the development of an indicator model to assess it, which is based on local data. The parameters included in this model are the joint persistence, the density of scars, the differential erosion, the number of points with potential rockfalls, and the slope mass rating SMR index.

For slow moving landslides with permanent or episodic activity, the landslide velocity was found to correlate well with the visible damage on the road pavement. The monthly thresholds of 3 and 10 mm and the cumulative displacement of 30 and 100 mm were used for the landslide intensity classification (see Table 13).

The highest risks in the study area referring to the repair cost for the damage of roads, are, in most cases associated, in descending order, with retaining structures, slow moving landslides, and rockfalls. The annual repair cost for retaining wall failure presents large variation for the different PoR, ought to the variation on the maintenance conditions and working loads. Using the proposed procedure, the prioritization of interventions for all the PoR was made and the number and location of the PoR that require imminent interventions can be assessed. The thresholds defining the risk classes can be adjusted, according to the financial availability for interventions, so as to point a smaller or higher number of PoR.

Several limitations exist in the application of the methodology which are related to the availability of data in the area, as well as the data quality. For slow moving landslides, the assessment of the temporal probability of reactivation is evidence-based, upon displacement measurements, and does not take directly into consideration specific landslide mechanisms, material behaviour, infiltration or groundwater variations, with the uncertainties that this implies. In the case of landslides with movement patterns that cannot be correlated to rainfall precipitation, the lack of knowledge for the causes of the acceleration is penalized by attributing to the PoR higher temporal probabilities of acceleration. Still, this leads to the estimation of an approximate probability rather than to a direct calculation of it. The overall coherent results between movement rate and visible road damage have served as a starting point for the risk analysis here. Nevertheless, in the event of not apparent correlation between the two or of velocity variations within the landslide body, further geotechnical studies are needed in order to study the effect of movement rate on the road. In the study area, slow moving landslides are well identified through prior geological and geotechnical studies for the detection of the fracture/sliding surface and the back analysis of the stability, hence deeper not monitored sliding surfaces would be exceptional. The identification of the landslide depth for the exclusion of deeper not monitored movements is a prerequisite for the proposed procedure, and is recommended for similar applications.

Given the inherent data and approach uncertainties, it is recommended that the final results are treated as relative and not as absolute ones. Further validation and refinement, using real annual costs is necessary for improving the method, which can be realized if repair cost data is systematically collected. This is an on-going procedure, as in the study area inspections are made periodically for the PoR with the higher risk rates, and landslide activity or damage are being assessed on a continuous basis, especially after extreme rainfall events. Towards this direction and on a long term basis, advanced monitoring techniques (e.g. use of SAR techniques, LiDAR…) with high temporal resolution and precision, as well as detailed water content measurements, could serve for the validation of the proposed procedure.

The calculated risk results are conservative, as in reality low and moderate damage is not repaired each time it occurs, but in larger time intervals. The inclusion of this parameter cannot be standardized for the study area, as the repair works are not regular.

As described in the introduction, the methodology developed here had as a starting point the requirements and data availability in the selected case study. Several parts of the proposed procedure for the risk assessment and ranking along road networks are strongly related to local conditions, concerning geological, geomorphological and climatic parameters and are empirical. Accordingly, the thresholds that have been selected here for the hazard descriptors and the classification of the consequences strongly depend on the expected range of frequency and magnitude/intensity of events in the study area. Moreover, the selection, scoring and weighting of the factors which are used for the calculation of the risk components are based on data collected in the study area, and as such, their use, although supported by the physical interpretation of the phenomena, can only become acceptable for the specific case study and cannot be transferred to other areas, without further studies. In that sense, the application of the proposed methodology to other case studies is principally suggested in terms of procedure and factors to consider for a multi-hazard integrated risk assessment for roadways. Adaptation to the local conditions is needed for the scoring, and classification of the hazard parameters, and for the assessment of temporal probability values considering the intensity and recurrence of local triggering factors, as well as for the asset and cost assessments. Further applications of the procedure presented here to areas with similar or diverse data settings would be useful for its refinement, and would provide an insight for framing the conditions of its transferability.

Acknowledgments

This work has been performed with the support of project on Integrated Assessment of the Geotechnical Risk of the Gipuzkoa road network (15-ES-563/2009) funded by the Gipuzkoako Foru Aldundia and of the Project RockModels-Caracterización y modelización de los desprendimientos rocosos (https://rockmodels.upc.edu/en) funded by the Spanish Ministry of Economy (Ref. BIA2016-75668-P, AEI/FEDER,UE).

References

Ábalos, B.: Geologic map of the Basque-Cantabrian Basin and a new tectonic interpretation of the Basque Arc, Int J Earth Sci (Geol Rundsch), 105, 2327, doi:10.1007/s00531-016-1291-6, 2016.

Barnolas, A, and Pujalte V: La Cordillera Pirenaica: definición, límites y división. In: Vera JA (ed) Geología de España, Sociedad Geológica de España—Instituto Geológico y Minero de España, Madrid, 233–241, 2004.

Budetta, P.: Assessment of rockfall risk along roads, Nat Hazard Earth Sys, 4(1), 71–81, doi: 10.5194/nhess-4-71-2004, 2004.

Bunce, C. M., Cruden, D. M., and Morgenstern, N. R.: Assessment of the hazard from rock fall on a highway, Can Geotech J, 34(3), 344–356, doi: 10.1139/cgj-34-3-344, 1997.

Corominas, J., van Westen, C., Frattini, P., Cascini, L., Malet, J. P., Fotopoulou, S. Catani, F. Van Den Eeckhaut, M., Mavrouli, O., Agliardi, F., and Pitilakis, K., Winter, M. G., Pastor, M., Ferlisi, S., Tofani, V., Hervás, J., Smith, J.T.: Recommendations for the quantitative analysis of landslide risk, B Eng Geol Environ, 73(2), 209-263, doi:10.1007/s10064-013-0538-8, 2014.

Dai, F., Lee, C., and Ngai, Y.: Landslide risk assessment and management: an overview, Eng Geol, 64(1), 65–87, doi:10.1016/S0013-7952(01)00093-X, 2002.

Eidsvig, U.M.K., Kristensen, K., and Vangelsten, B.V.: Assessing the risk posed by natural hazards to infrastructures, Nat Hazard Earth Sys, 17, 481–504, doi:10.5194/nhess-17-481-2017, 2017.

Fell, R., Corominas, J., Bonnard, C., Cascini, L., Leroi, E., and Savage, W. Z.: Guidelines for landslide susceptibility, hazard and risk zoning for land use planning, Eng Geol, 102, 85–98. doi: 10.1016/j.enggeo.2008.03.022, 2008.

Ferlisi, S., Cascini, L., Corominas, J., Matano, F.: Rockfall risk assessment to persons travelling in vehicles along a road: the case study of the Amalfi coastal road (southern Italy), Nat Hazards, 62, 691–721, doi: 10.1007/s11069-012-0102-z, 2012.

Ferrero, A. M., and Migliazza, M.: Landslide Transportation Network and Lifelines: Rockfall and Debris Flow. In Landslide Science and Practice, Berlin, Heidelberg: Springer Berlin Heidelberg, 161–170, doi: 10.1007/978-3-642-31319-6_23, 2013.

Gharaibeh, N. G., and Lindholm, D.: A condition assessment method for roadside assets. Struct Infrastruct E, 10(3), 409-418, https://doi.org/10.1080/15732479.2012.757330, 2014.

Gómez, M., Vergés, J., Riaza, C.: Inversion tectonics of the northern margin of the Basque Cantabrian Basin, B Soc Geol Fr, 173:449–459, doi: 10.2113/173.5.449, 2002.

Hungr, O., Evans, S. G., and Hazzard, J.: Magnitude and frequency of rock falls and rock slides along the main transportation corridors of southwestern British Columbia, Can Geotech J, 36(2), 224–238, doi:10.1139/t98-106, 1999.

Jaiswal, P., Van Westen, C. J., and Jetten, V.: Quantitative landslide hazard assessment along a transportation corridor in southern India, Eng Geol, doi:10.1016/j.enggeo.2010.09.005, 2010.

Kappes, M.S., Gruber, K., Frigerio, S., Bell, R., Keiler, M., Glade, T. The MultiRISK platform: The technical concept and application of a regional-scale multihazard exposure analysis tool. Geomorphology 151–152: 139-155. doi.org/10.1016/j.geomorph.2012.01.024, 2012.

Mansour, M. F., Morgenstern, N. R., and Martin, C. D.: Expected damage from displacement of slow-moving slides. Landslides, 8(1), 117–131, doi:10.1007/s10346-010-0227-7, 2011.

Michoud, C., Derron, M.-H., Horton, P., Jaboyedoff, M., Baillifard, F.-J., Loye, A., Nicolet, P., Pedrazzini, A., and Queyrel, A.: Rockfall hazard and risk assessments along roads at a regional scale: example in Swiss Alps, Nat Hazard Earth Sys, 12, 615–629, doi: 10.5194/nhess-12-615-2012, 2012.

Nicolet, P., Jaboyedoff, M., Cloutier, C., Crosta, G. B., and Lévy, S.: Brief communication: On direct impact probability of landslides on vehicles, Nat Hazard Earth Sys, 16(4), 995-1004, 2016.

Pantelidis, L.: A critical review of highway slope instability risk assessment systems, B Eng Geol Environ, 70(3), 395–400, doi: 10.1007/s10064-010-0328-5, 2011.

Pellicani, R., Argentiero, I., and Spilotro, G.: GIS-based predictive models for regional-scale landslide susceptibility assessment and risk mapping along road corridors, Geomat Nat Haz Risk, 1–22, doi: 10.1080/19475705.2017.1292411, 2017.

Pierson L.A. and Van Vickle, R.: Rockfall Hazard Rating System. Publication No. FHWA SA-93. U.S. Department of Transportation. Fedeal Highway Administration. Retrieved from http://www.dot.ca.gov/hq/esc/geotech/references/Rockfall_References/30_Pierson_Rockfall_Hazard_Rating_System.pdf (last accessed 3 August 2018), 1993.

Remondo, J., Bonachea, J., and Cendrero, A.: Quantitative landslide risk assessment and mapping on the basis of recent occurrences, Geomorphology, 94(3–4), 496–507, doi: 10.1016/j.geomorph.2006.10.041, 2008.

Romana, M.: SMR classification. In: International Society of Rock Mechanics (ed) Proceedings 7th International Congress on Rock Mechanics, Aachen, Germany, Balkema, Rotterdam, 2, 955-960, 1991.

Schmidt, J., Matcham, I., Reese, S., King, A., Bell, R., Henderson, R., Smart, G., Cousins, J., Smith, W., Heron, D. Quantitative multi-risk analysis for natural hazards: a framework for multi-risk modelling, Natural Hazards 58 (3): 1169- 1192. doi.org/10.1007/s11069-011-9721-z, 2011

Silva, F., Lambe, T. W., and Marr, W. A.: Probability and Risk of Slope Failure, J Geotech Geoenviron, 34(12), 1691–1699, doi:10.1061/(ASCE)1090-0241(2008)134:12(1691), 2008.

Tugend, J., Manatschal, G., Kuzsnir, N.J., Masini, E., Mohn, G., and Thinon I: Formation and deformation of hyperextended rift systems: insights from rift domain mapping in the Bay of Biscay-Pyrenees, Tectonics, 33,1239–1276, doi: 10.1002/2014TC003529, 2014.

Vega, J. A., and Hidalgo, C. A.: Quantitative risk assessment of landslides triggered by earthquakes and rainfall based on direct costs of urban buildings. Geomorphology, 273, 217-235, doi: 10.1016/j.geomorph.2016.07.032, 2016.

Zêzere, J. L., Garcia, R. A. C., Oliveira, S. C., and Reis, E.: Probabilistic landslide risk analysis considering direct costs in the area north of Lisbon (Portugal), Geomorphology, 94(3–4), 467–495, doi: 10.1016/j.geomorph.2006.10.040, 2008.

Appendix - Table 13: Consequence classification and costs for each hazard type (source of costs Ikerlur and Gipuzkoako Foru Aldundia).

Hazard type and variable for consequence classification	Class	Principal consequences and disruption	Actions	Cost (in UC)
RF - Rockfall magnitude (m^3)	A (<1)	platform not/partially occupied, no/partial disruption	(Alternative pass + removal debris)	0.8
	B (1-5)	platform partially occupied, partial disruption	(Alternative pass) + removal debris	1.5
	C (5-50)	platform occupied, disruption	Alternative pass + removal debris	3.9
	D (50-500)	platform occupied, disruption	Interruption road + removal debris + slope scaling	17.5
	E (50-5,000)	platform occupied and damaged, disruption	Interruption road + removal debris + repair road + intensive scaling	117.2
	F (>5,000)	platform occupied and damaged, disruption	Interruption road + removal debris + repair road + intensive scaling	172.4
RS - Wall structure failure extent	Partial failure of small wall	no damage, no/partial disruption	Removal + slope scaling	20.9 (per 10 m wall)
	Height wall: ≤ 6 m	platform occupied and damaged, disruption	Removal + slope scaling + stabilization + reconstruction wall + repair road	70.3 (per 10 m wall)
	Height wall: > 6 m	platform occupied and damaged, disruption	Removal + slope scaling stabilization + reconstruction wall + repair road	121.0 (per 10 m wall)
SL - Max rate of terrain displacement (mm/month) and instability indicators	$v_A < 3$	Without/slight damage, no disruption	Repair road	1.4 (per 10 m damaged road)
	$3 < v_B < 10$	Moderate damage, no disruption	Repair road	15.0 (per 10 m damaged road)
	$v_C > 10$	Severe damage, no/partial disruption	Repair road + stabilization	37.4 (per 10 m damaged road)
	$v_D > 10$ and presence of scarp or developed shear displacements	Partial/total destruction, disruption	Interruption road + scaling slope + stabilization	45.4 (per 10 m damaged road)